

Extraction of the pion-nucleon coupling constant using the effective-range expansion with the left-hand cut

Bo-Yang Liu,^{1,2} Bing Wu^{3,*} Ji-Wei Fu,³ Meng-Lin Du^{3,†}

Feng-Kun Guo^{1,2,4,‡} and Ulf-G. Meißner^{5,6,7,§}

¹*Institute of Theoretical Physics, Chinese Academy of Sciences, Beijing 100190, China*

²*School of Physical Sciences, University of Chinese Academy of Sciences, Beijing 100049, China*

³*School of Physics, University of Electronic Science and Technology of China, Chengdu 611731, China*

⁴*Southern Center for Nuclear-Science Theory (SCNT), Institute of Modern Physics,
Chinese Academy of Sciences, Huizhou 516000, China*

⁵*Helmholtz-Institut für Strahlen- und Kernphysik and Bethe Center
for Theoretical Physics, Universität Bonn, D-53115 Bonn, Germany*

⁶*Institute for Advanced Simulation (IAS-4), Forschungszentrum Jülich, D-52425 Jülich, Germany*

⁷*Peng Huanwu Collaborative Center for Research and Education, International Institute
for Interdisciplinary and Frontiers, Beihang University, Beijing 100191, China*

We apply the generalized effective-range expansion of Ref. [1] (Phys. Rev. Lett. 135, 011903 (2025)), which incorporates the left-hand cut from one-pion exchange, to low-energy neutron–proton scattering in the 1S_0 and 3S_1 channels. The amplitude zero for the center-of-mass momentum near 0.35 GeV in the 1S_0 channel is naturally accommodated within this framework. We extract the pole position, scattering length, effective range, and the pseudoscalar pion–nucleon coupling constant $g_{\pi N}^2/(4\pi)$ at different expansion orders. The low-energy parameters are stable and consistent with established values, while $g_{\pi N}^2/(4\pi)$ exhibits larger uncertainties. The extraction of $g_{\pi N}^2/(4\pi)$ is data-driven, relying on the analytic constraints from the left-hand cut and phase-shift data within the one-pion-exchange approximation. Despite larger uncertainties compared to high-precision extractions, the consistency with established values demonstrates that this framework can probe the left-hand-cut singularity.

* wu.bing@uestc.edu.cn

† du.ml@uestc.edu.cn

‡ fkguo@itp.ac.cn

§ meissner@hiskp.uni-bonn.de

I. INTRODUCTION

The effective range expansion (ERE) [2, 3] provides a model-independent parameterization of the low-energy two-body scattering amplitude, based on unitarity and analyticity, and has been widely employed in the analysis of near-threshold phenomena. Its importance has grown significantly in recent decades with the discovery of numerous exotic hadronic states and candidates located close to two-body thresholds [4–12]. For two-particle S -wave scattering in relativistic kinematics, the unitarized amplitude takes the form

$$T(s) = 8\pi\sqrt{s}f(s) = \frac{8\pi\sqrt{s}}{k \cot \delta - ik} . \quad (1)$$

With this convention, the S -wave amplitude f has the dimension of length. Here, s is the center-of-mass (c.m.) energy squared, k is the magnitude of the momentum of either particle in the c.m. frame, and δ is the phase shift. The conventional ERE expands $k \cot \delta$ as a power series in k^2 in the near-threshold region:

$$k \cot \delta = \frac{1}{a} + \frac{1}{2}rk^2 + \mathcal{O}(k^4) , \quad (2)$$

which defines the scattering length a and effective range r , with the sign of the first term being convention-dependent. The unitarity cut is isolated in the ik term in Eq. (1) and $k \cot \delta$ is free of singularities in the vicinity of the threshold. The radius of convergence of the Taylor-series expansion in Eq. (2) is limited by the location of the nearest singularity in the complex energy plane. When the exchanged particle is relatively light for the t -channel exchange (or only slightly heavier than the mass difference of the two scattering particles for the u -channel exchange), the branch point of the left-hand cut (lhc) can lie close to the threshold, severely restricting the convergence domain of Eq. (2) [1, 13]. See also Ref. [14] for a pedagogical introduction.

To systematically incorporate such a near-threshold lhc, a generalized ERE was recently proposed in Ref. [1],¹ given by

$$k \cot \delta = \frac{\tilde{d}(k^2) - \tilde{g}d^R(k^2)}{\tilde{n}(k^2) + \tilde{g}[L(k^2) - L(0)]} , \quad (3)$$

where $\tilde{d}(k^2)$ and the normalized $\tilde{n}(k^2)$ are polynomials in k^2 . The logarithmic functions $d^R(k^2)$ and $L(k^2)$, which are given below, encapsulate the analytic structure introduced by the lhc, while the parameter \tilde{g} quantifies its contribution and encodes the coupling strength to the exchanged

¹ The reliability and a higher-order improvement of this scheme, along with a kinematically relativistic version, have been addressed in Ref. [15].

particle. Since the discontinuity of the amplitude across the one-particle exchange lhc originates from the corresponding tree-level exchange diagram, one can extract the coupling strength of the scattering particles to the exchanged particle from the generalized ERE (3), as demonstrated for the case of $D^*D\pi$ coupling at an unphysical pion mass in Ref. [1]. Furthermore, under certain conditions, the generalized ERE can naturally accommodate an amplitude zero, corresponding to a pole of $k \cot \delta$. Since its location can be expressed in terms of ERE parameters and the mass and coupling of the long-range exchanged particle, the corresponding amplitude zero can be understood as arising from an interplay between the short-range and long-range forces [1], as seen in Ref. [16] for neutron–one-neutron-halo-nucleus scattering and in Ref. [17] for DD^* scattering. This feature is inherent to the framework. In contrast, the conventional ERE (2) lacks such zeros unless augmented by additional Castillejo-Dalitz-Dyson (CDD) poles; however, the connection to the long-range force is missing. Such a near-threshold amplitude zero potentially offers a promising testbed for validating this scheme. Over the past several decades, experimental and theoretical studies of the 1S_0 neutron-proton (np) phase shift have consistently indicated the presence of an amplitude zero (corresponding to the point $\delta = 0$) near $k \simeq 0.35$ GeV, as illustrated in Fig. 1. Given the presence of both one-pion exchange (OPE) as a long- but finite-range interaction and shorter-range forces, the nucleon–nucleon (NN) scattering is an ideal case to apply and test the generalized ERE of Eq. (3).

This framework has been successfully applied to reproduce the DD^* scattering amplitudes obtained from the Lippmann-Schwinger equation (LSE) and to extract the axial-vector $D^*D\pi$ coupling constant [1]. It should be noted that in that work, the fit to the LSE amplitude employed six equidistant pseudo-data points, three of which lie on the lhc, including one very close to the lhc branch point. However, since experimental data are confined to the physical region above the threshold, critical questions arise: If only such physical-region data are available, how reliable is this parameterization? To what extent can the coupling constants be accurately extracted?

In this work, we analyze low-energy NN scattering phase shifts in the physical region using the generalized ERE, Eq. (3), with particular attention to the 1S_0 np channel. We extract the pseudoscalar πNN coupling constant, as well as the pole position, scattering length, and effective range. We compare the results across different expansion orders with established determinations in the literature to assess the stability of the extraction. The paper is organized as follows. After this Introduction, we present the theoretical formalism in Sec. II. This includes a detailed derivation of the generalized ERE for completeness in Sec. II A, the construction of the NN scattering potential in Sec. II B, and the definitions of physical parameters in Sec. II C. The fitting of experimental NN

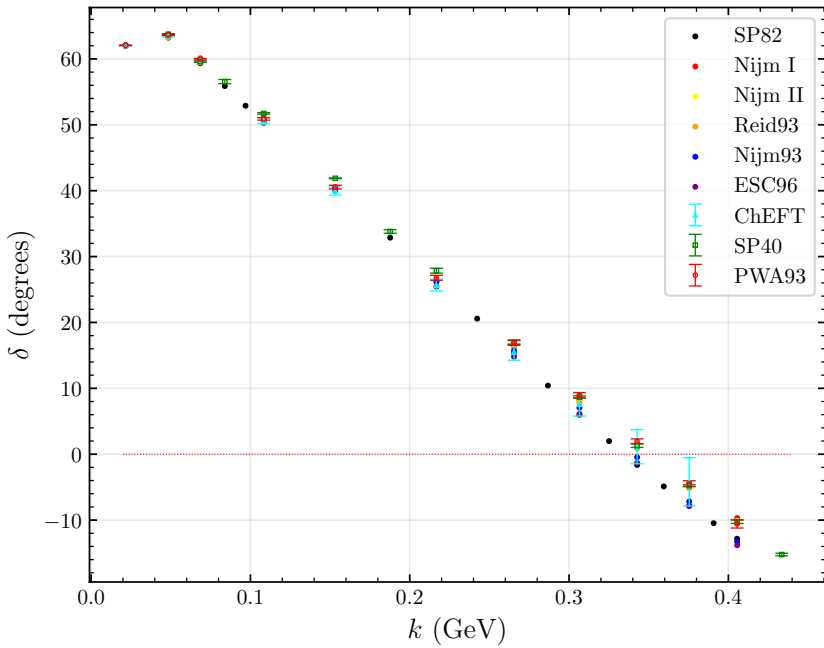


FIG. 1. 1S_0 np scattering phase shift. Data points are from the following references: SP82 (Ref. [18]), Nijm I, Nijm II, Reid93, and Nijm93 (Ref. [19]), ESC96 (Ref. [20]), ChEFT (Ref. [21]), SP40 (Ref. [22]), and PWA93 (Ref. [23]).

data with the generalized ERE at different orders is discussed in Sec. III. The paper concludes with a brief summary in Sec. IV.

II. FORMALISM

A. ERE with the lhc

For S -wave elastic scattering, the contribution from the t -channel one-particle exchange lhc is given by [1]

$$L(k^2) \equiv \frac{1}{2} \int_{-1}^{+1} \frac{d \cos \theta}{t - m_{\text{ex}}^2} = -\frac{1}{4k^2} \log \frac{m_{\text{ex}}^2/4 + k^2}{m_{\text{ex}}^2/4}, \quad (4)$$

where m_{ex} denotes the mass of the exchanged particle.² The branch point of the lhc is located at $k_{\text{lhc}}^2 = -m_{\text{ex}}^2/4$. This implies that a larger exchanged-particle mass places the branch point farther from threshold, thereby reducing the influence of this singularity on the physical region within the

² In this work, isospin-breaking effects between protons and neutrons are neglected, rendering the partial-wave amplitudes of the u - and t -channels identical.

dispersion-relation framework. Therefore, in the subsequent analysis, we restrict ourselves to OPE and neglect contributions from heavier exchanges such as S -wave two pions (or σ in the one-boson exchange model), ρ , and ω mesons.

To simultaneously incorporate both the OPE lhc and the unitarity cut, the formalism of Ref. [1] starts with the N/D method [24, 25], in which the scattering amplitude is written as

$$f(k^2) = \frac{n(k^2)}{d(k^2)}, \quad (5)$$

where the numerator $n(k^2)$ contains only the lhc and the denominator $d(k^2)$ contains only the unitarity cut. Using dispersion relations, these functions can be expressed as [1]

$$n(k^2) = \tilde{n}(k^2) + \tilde{g}(L(k^2) - L_0), \quad (6)$$

$$d(k^2) = \tilde{d}(k^2) - ikn(k^2) - \tilde{g}d^R(k^2), \quad (7)$$

where $\tilde{n}(k^2)$ and $\tilde{d}(k^2)$ are rational functions of k^2 in general. The parameter \tilde{g} , together with $L_0 = L(k^2 = 0) = -1/m_{\text{ex}}^2$, is chosen so that $n(k^2)$ is normalized at threshold, i.e., $\tilde{n}(0) = 1$. The function $d^R(k^2)$, which cancels the lhc contribution from $-ikn(k^2)$ and ensures that $d(k^2)$ is free of the lhc, is given by

$$d^R(k^2) = \frac{i}{4k} \log \frac{m_{\text{ex}}/2 + ik}{m_{\text{ex}}/2 - ik}. \quad (8)$$

Expanding $\tilde{n}(k^2)$ and $\tilde{d}(k^2)$ as polynomials of orders m and n , respectively, the scattering amplitude can be parameterized as

$$\frac{1}{f_{[m,n]}(k^2)} = \frac{\sum_{i=0}^n \tilde{d}_i k^{2i} - \tilde{g}d^R(k^2)}{1 + \sum_{j=1}^m \tilde{n}_j k^{2j} + \tilde{g}(L(k^2) - L_0)} - ik, \quad (9)$$

where $\tilde{d}_i, i = 0, \dots, n$, and $\tilde{n}_j, j = 1, \dots, m$, are the expansion coefficients. Comparing with the parameterization of the scattering amplitude in Eq. (1), we obtain [1]:

$$k \cot \delta = \frac{\sum_{i=0}^n \tilde{d}_i k^{2i} - \tilde{g}d^R(k^2)}{1 + \sum_{j=1}^m \tilde{n}_j k^{2j} + \tilde{g}(L(k^2) - L_0)}. \quad (10)$$

B. The S -wave NN OPE potential and unitarized amplitude

The Lagrangian for the pseudoscalar form of the πNN coupling, together with the nucleon kinetic and mass terms, is given by

$$\mathcal{L}_{\pi NN} = \bar{N}(i\gamma^\mu \partial_\mu - m_N)N + ig_{\pi N}\bar{N}\gamma_5 \vec{\tau} \cdot \vec{\pi}N, \quad (11)$$

where m_N is the isospin-averaged nucleon mass,³ $g_{\pi N}$ is the pseudoscalar pion-nucleon coupling constant, and $\vec{\tau}$ denotes the Pauli matrices in the isospin space. The isospin multiplets are defined as

$$N = \begin{pmatrix} p \\ n \end{pmatrix}, \quad \vec{\pi} = \left(\frac{\pi^+ + \pi^-}{\sqrt{2}}, \frac{\pi^- - \pi^+}{i\sqrt{2}}, \pi^0 \right). \quad (12)$$

Alternatively, the πNN coupling can take a derivative form to reflect the fact that pions are pseudo-Nambu-Goldstone bosons of the spontaneous chiral symmetry breaking, for which the standard leading-order SU(2) chiral Lagrangian for the πN interaction gives

$$\mathcal{L}_{\pi N}^{(1)} = \frac{g_A}{2} \bar{N} \gamma^\mu \gamma_5 u_\mu N, \quad (13)$$

where g_A denotes the nucleon axial-vector coupling constant in the chiral limit. The chiral vielbein is defined as

$$u_\mu = iu^\dagger \partial_\mu u - iu \partial_\mu u^\dagger, \quad (14)$$

with $u^2 = U$ and $U = \exp(i\vec{\tau} \cdot \vec{\pi}/F_\pi)$, where F_π is the pion decay constant in the chiral limit. The πNN couplings in the Lagrangians (11) and (13) for on-shell particles are equivalent, and the coupling constants are related to each other by the Goldberger-Treiman relation, $g_{\pi N} = g_A m_N / F_\pi$ [26]. Corrections to this relation are small; see, e.g., Ref. [27].

From the Lagrangian (11), the tree-level OPE amplitude⁴ in the c.m. frame as shown in Fig. 2 reads

$$V(\vec{q}) = g_{\pi N}^2 \vec{\tau}_1 \cdot \vec{\tau}_2 \frac{\vec{\sigma}_1 \cdot \vec{q} \vec{\sigma}_2 \cdot \vec{q}}{\vec{q}^2 + M_\pi^2}, \quad (15)$$

where M_π is the isospin-averaged pion mass, $\vec{\sigma}_i$ ($\vec{\tau}_i$) is the spin (isospin) Pauli matrix of nucleon i , and \vec{q} is the three-momentum transferred by the pion. Using the SU(2) Clebsch–Gordan coefficients, the isospin factor evaluates to

$$\langle I_f | \vec{\tau}_1 \cdot \vec{\tau}_2 | I_i \rangle = (2I_f(I_f + 1) - 3) \delta_{I_f I_i}, \quad (16)$$

where I_i and I_f denote the total isospin of the initial and final two-nucleon states, respectively. For S -wave scattering, the spin-dependent term upon angular averaging simplifies as

$$\vec{\tau}_1 \cdot \vec{q} \vec{\tau}_2 \cdot \vec{q} \rightarrow \frac{\vec{\sigma}_1 \cdot \vec{\sigma}_2}{3} \vec{q}^2. \quad (17)$$

³ Strictly speaking, the chiral limit values of the various parameters appear here, but to the order we are working, we can equate these with their physical values.

⁴ In the c.m. frame, the t -channel momentum transfer is purely spatial, $q = (0, \vec{q})$, the amplitude reduces to the three-dimensional form given in Eq. (15).

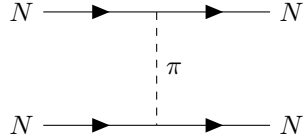


FIG. 2. Feynman diagram for the $NN \rightarrow NN$ process with OPE.

This follows from $\langle q_i q_j \rangle_\Omega = \frac{1}{3} \vec{q}^2 \delta_{ij}$ for an S -wave angular average. Due to the Pauli exclusion principle, the total (isospin, spin) of an S -wave NN system could be either (1,0) or (0,1). As a consequence, the states $|^1S_0, I = 1\rangle$ and $|^3S_1, I = 0\rangle$ experience the same potential

$$V_0(k^2) = -g_{\pi N}^2 M_\pi^2 L(k^2), \quad (18)$$

where the subscript 0 indicates the S -wave. For the 1S_0 ($I = 1$) and 3S_1 ($I = 0$) channels, the spin-isospin factor yields the same projected OPE kernel $V(\vec{q}) = -g_{\pi N}^2 \vec{q}^2 / (\vec{q}^2 + M_\pi^2)$. Writing $\vec{q}^2 / (\vec{q}^2 + M_\pi^2) = 1 - M_\pi^2 / (\vec{q}^2 + M_\pi^2)$, the first term is a short-range contact interaction (omitted here), while the second term gives Eq. (18) after the S -wave projection with $t = -\vec{q}^2$. Note that $L(0) \neq 0$; however, in the N/D representation the lhc contribution enters through the subtracted combination $L(k^2) - L_0$ in Eq. (6), which fixes the threshold normalization and does not affect the lhc discontinuity determined by $\text{Im } L(k^2)$. Starting from this tree-level OPE and contact potentials, the unitarized amplitude $T(k^2)$ can be obtained by solving the LSE. Noting that the discontinuity of the amplitude across the one-particle exchange lhc originates from the corresponding tree-level exchange diagram, we obtain [1]

$$\text{Im}T(k^2) = 8\pi\sqrt{s} \text{Im}f(k^2) = \text{Im}V_0(k^2), \quad \text{for } k^2 \leq k_{\text{lhc}}^2. \quad (19)$$

C. Extraction of low-energy parameters

Now we can relate the generalized ERE with lhc and OPE potential to extract the coupling constant following Ref. [1]. From Eqs. (5, 6) and noting that $d(k^2)$ is free of the lhc, we obtain

$$\text{Im}f(k^2) = \frac{\tilde{g} \text{Im}L(k^2)}{d(k^2)}, \quad \text{for } k^2 \leq k_{\text{lhc}}^2. \quad (20)$$

Combining Eqs. (18, 19) and restricting our analysis to the near-threshold region, we obtain

$$\frac{g_{\pi N}^2}{4\pi} = -\frac{\tilde{g}}{d^{0,\text{lhc}}} \frac{4m_N}{M_\pi^2}, \quad (21)$$

where $d^{0,\text{lhC}}$ denotes the value of $d(k^2)$ at the branch point of the lhC, i.e.,

$$d^{0,\text{lhC}} = \sum_{i=0}^n \tilde{d}_i \left(\frac{-m_{\text{ex}}^2}{4} \right)^i + \frac{m_{\text{ex}}}{2} \left(1 + \sum_{j=1}^m \tilde{n}_j \left(\frac{-m_{\text{ex}}^2}{4} \right)^j + \frac{\tilde{g}}{m_{\text{ex}}^2} \right) + \frac{\tilde{g} \log 2}{m_{\text{ex}}}. \quad (22)$$

This expression is obtained by evaluating Eq. (7) in the limit $k^2 \rightarrow -m_{\text{ex}}^2/4$ (i.e., $k \rightarrow im_{\text{ex}}/2$), where the logarithmic singularities in $-ikn(k^2)$ and $d^R(k^2)$ cancel, leaving the finite $\log 2$ term; see Ref. [1] for details.

Furthermore, from Eqs. (2, 10), the S -wave scattering length a and effective range r can be extracted directly as

$$\begin{aligned} a &= f(k^2 = 0) = \left(\tilde{d}_0 + \frac{\tilde{g}}{m_{\text{ex}}} \right)^{-1}, \\ r &= 2 \frac{d}{d(k^2)} \left(\frac{1}{f} + ik \right) \Big|_{k^2=0} = 2\tilde{d}_1 - \frac{8\tilde{g}}{3m_{\text{ex}}^3} - \left(2\tilde{n}_1 + \frac{4\tilde{g}}{m_{\text{ex}}^4} \right) \frac{1}{a}. \end{aligned} \quad (23)$$

The coefficients in the effective-range expression follow from the threshold expansions of Eqs. (4, 8):

$$L(k^2) = -\frac{1}{m_{\text{ex}}^2} + \frac{2k^2}{m_{\text{ex}}^4} + \mathcal{O}(k^4), \quad d^R(k^2) = -\frac{1}{m_{\text{ex}}} + \frac{4k^2}{3m_{\text{ex}}^3} + \mathcal{O}(k^4).$$

Expanding Eq. (10) to $\mathcal{O}(k^2)$ and using $k \cot \delta = 1/f + ik$ then reproduces the numerical coefficients $8/3$ and 4 in the last line above.

III. RESULTS AND DISCUSSION

Using the np scattering phase shifts from Ref. [23],⁵ which provide the data below 350 MeV for the kinetic energy in the laboratory frame and serve as a benchmark in chiral nuclear force studies (see, e.g., Refs. [29–31]), we perform fits with the generalized ERE as given in Eq. (10). As mentioned above, it allows us to extract the low-energy parameters for the NN system, including the pseudoscalar coupling constant, pole position, scattering length, and effective range, and it also serves to test the stability of the present parameterization scheme. Two different fitting strategies are employed. In the first strategy, we fit the phase shifts of the independent channels $|^1S_0, I = 1\rangle$ and $|^3S_1, I = 0\rangle$ (the deuteron channel) separately.⁶ The second strategy consists in performing a

⁵ We use np rather than proton-proton (pp) scattering data because the latter involves additional Coulomb effects [28] that fall outside the present theoretical framework.

⁶ The effects of the S - D mixing due to the tensor force, via the term $\vec{\sigma}_1 \cdot \vec{q} \vec{\sigma}_2 \cdot \vec{q}$ in Eq. (15), are neglected in this analysis because the D -state probability in the deuteron is only about 5% [32] and does not affect the location of the lhC branch point.

combined analysis by fitting to both channels simultaneously while incorporating the high-precision experimental measurement of the bound coherent scattering length

$$a_c = \left(1 + \frac{m_n}{m_p}\right) \frac{1}{4} (3a_{|3S_1\rangle} + a_{|1S_0\rangle}), \quad (24)$$

where m_n and m_p denote the neutron and proton masses, respectively. The prefactor $(1 + m_n/m_p)$ accounts for the standard conversion between the c.m. and laboratory definitions of the bound coherent scattering length. In the isospin-symmetric approximation $m_n = m_p$ adopted in this work, Eq. (24) reduces to $a_c = \frac{1}{2}(3a_{|3S_1\rangle} + a_{|1S_0\rangle})$. A quantitative estimate of isospin-breaking corrections to this constraint is beyond the scope of the present work. We take $a_c = 3.7384(20)$ fm from Ref. [33].⁷

A. Channel-by-channel Fit

An excellent description of the $|^1S_0, I = 1\rangle$ channel phase shift is achieved with the [1, 2] order parametric scheme⁸ in Eq. (9). The extracted parameters, a virtual pole at $-66.4^{+0.6}_{-0.5}$ keV on the unphysical Riemann sheet, a scattering length of $23.72^{+0.10}_{-0.08}$ fm, and an effective range of $2.68^{+0.02}_{-0.03}$ fm (row 5 of Table I), show excellent agreement with earlier results from Ref. [34–36] (rows 7 to 9), where the pole positions in Refs. [34–36] are derived from the conventional ERE [37] $E_{\text{pole}} = (1 - \sqrt{1 + 2r/a})^2/(r^2 m_N)$. The pseudoscalar coupling constant, $g_{\pi N}^2/(4\pi) = 12.4^{+2.2}_{-2.3}$, also falls within the accepted range and is compatible with previous determinations [38–42] (rows 12 to 16) within the conditional uncertainties discussed above. In particular, the amplitude zero, corresponding to a pole of $k \cot \delta$, at around $k = 0.35$ GeV, see Fig. 3, is properly produced.

For the $|^3S_1, I = 0\rangle$ channel, the [2, 1] parametric scheme provides a good description of the data, yielding a bound pole at -2222^{+14}_{-12} keV, a scattering length of $-5.416^{+0.002}_{-0.003}$ fm, and an effective range of $1.749(7)$ fm (row 6 of Table I), in good agreement with earlier studies [23, 34–36, 43] (rows 7 to 11). In contrast, the pseudoscalar coupling constant exhibits a larger uncertainty, specifically $g_{\pi N}^2/(4\pi) = 18.3^{+8.4}_{-8.6}$. Nevertheless, within uncertainties, our extracted coupling remains consistent with previous determinations [38–42]. The large uncertainty shows that without the S - D mixing that arises from the OPE tensor force, the sensitivity from only the S -wave phase shift to the OPE is weaker than that in the $|^1S_0, I = 1\rangle$ channel.

⁷ The sign of the coherent scattering length quoted in Ref. [33] has been converted to match the convention adopted in this work.

⁸ An almost equally good description of the phase shift can be achieved with the [2, 1] order parametrization, leading to consistent low-energy parameters and the pole position with the [1, 2] parameterization.

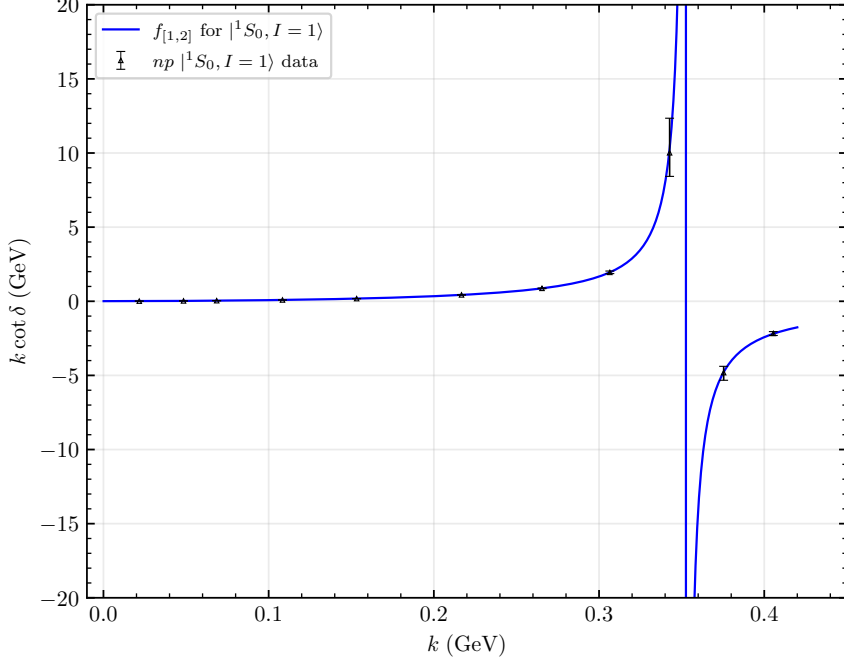


FIG. 3. Comparison of $k \cot \delta$ between the best fit and data for the $np |^1S_0, I = 1\rangle$ channel (fit performed with the generalized ERE (10) on scattering phase shift from Ref. [23]).

The extraction of the coupling constant $g_{\pi N}^2/(4\pi)$ provides a nontrivial consistency check of the OPE-driven lhc contribution within the generalized ERE framework, and shows that the framework can be used to probe couplings related to the one-particle exchange. In contrast to the low-energy parameters (a, r, E_{pole}), which are tightly constrained by the phase shifts, the uncertainty of $g_{\pi N}^2/(4\pi)$ is considerably larger, especially in the 3S_1 -only fit, reflecting that the sensitivity to the lhc is weaker since it is located in the unphysical region and is logarithmic.

B. Joint analysis of the 1S_0 and 3S_1 channels

In this subsection, we perform a joint analysis of both $|^1S_0, I = 1\rangle$ and $|^3S_1, I = 0\rangle$ channels under the constraint of the coherent scattering length $a_c = 3.7384(20)$ fm, defined in Eq. (24). While the expansion orders and the parameter values in Eq. (9) are different in general for the two channels, their long-range potentials are identical, as given in Eq. (18). This common long-range part implies that $\tilde{g}/d^{0,\text{lhc}}$ should be the same for the two channels, leading to the common $g_{\pi N}^2/(4\pi)$. Imposing this constraint together with the central value of the coherent scattering length, we fit the phase shifts of both channels using either the same or different expansion orders.

For comparison, four distinct parametrizations of Eq. (9) at different orders of the parametriza-

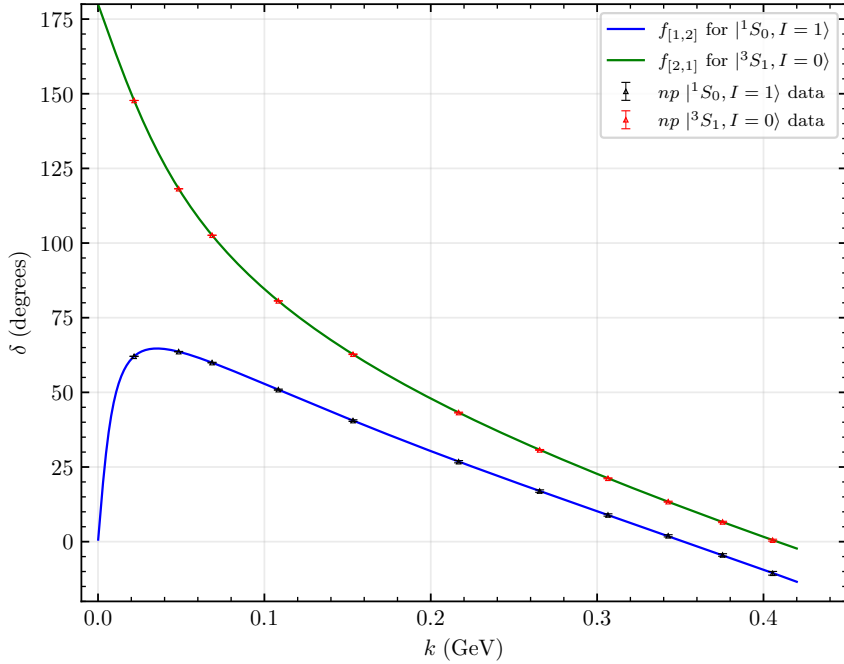


FIG. 4. Joint fit to the data from Ref. [23] using the generalized ERE in Eq. (10).

tion that provide a good description of the data are considered. As shown in the first four rows of Table I, all four sets yield highly consistent values for the pole positions, scattering lengths, effective ranges, and coupling constants. Within uncertainties, these results agree with previous determinations (last five rows of Table I). The extracted central values are stable across these parametrizations; however, the central value of the coupling constant tends to be smaller than several recent high-precision determinations. The corresponding fit results are displayed in Fig. 4. Only one representative parametrization is plotted, as the differences among the various schemes are visually indistinguishable. We have also varied the input coherent scattering length within its quoted uncertainty, $a_c = 3.7384(20)$ fm [33]. The resulting uncertainty propagated to $g_{\pi N}^2/(4\pi)$ was found to be extremely small (about 0.07), negligible compared to the statistical errors.

Table I also lists selected results for the pseudoscalar πN coupling from earlier studies. Our extracted values of $g_{\pi N}^2/(4\pi)$ fall into the broad range of existing determinations. Following Yukawa's theory, Bethe obtained $g_{\pi N}^2/(4\pi) = 14.56(28)^*$ ⁹ in 1940s by solving the Schrödinger equation for deuteron observables [44, 45]. Nambu later estimated a value around 13.5 using the Goldberger-Treiman relation [46, 47]. Through pion pole extrapolation of the renormalized Born approximation [48], analyses of np and pp scattering data yielded $g_{\pi N}^2/(4\pi) = 12.0(21)$ [49, 50]. Subsequent

⁹ Values marked with an asterisk are originally given in terms of $f_{\pi^a NN'}^2$, which relates to the pseudoscalar coupling via $g_{\pi^a NN'}^2/(4\pi) = f_{\pi^a NN'}^2(m_{N'} + m_N)^2/M_{\pi^\pm}^2$ (with $N, N' = n, p$ and $\pi^a = \pi^0, \pi^\pm$). As the relevant masses are not explicitly specified in the cited references, we convert these values using standard particle masses.

TABLE I. Extracted parameters for the NN $|^1S_0, I = 1\rangle$ and $|^3S_1, I = 0\rangle$ systems from a fit to the np scattering phase shifts of Ref. [23] using the ERE with lhc (10). The table lists the pole position, scattering length, effective range, pseudoscalar coupling constant, and $\chi^2/\text{d.o.f}$. The first four rows present a joint analysis of both channels with a common $g_{\pi N}^2/(4\pi)$ and the fixed bound coherent scattering length $a_c = 3.7384$ fm, taken from the central value reported in Ref. [33]. Results of independent fits to the $|^1S_0, I = 1\rangle$ and $|^3S_1, I = 0\rangle$ channels are shown separately in rows 5 and 6, respectively. For comparison, rows 7–16 list values obtained from other references. The sign of the scattering length quoted in Refs. [35, 36] has been converted to match the convention adopted in this work, i.e., $k \cot \delta = 1/a + \dots$ as in Eq. (2). The quoted pole positions refer to the first Riemann sheet for the $|^3S_1, I = 0\rangle$ state (the deuteron) and the second Riemann sheet for the $|^1S_0, I = 1\rangle$ state. Negative values of E_{pole} correspond to poles below the NN threshold.

ERE w/ lhc		E_{pole} (keV)		a (fm)		r (fm)		$\frac{g_{\pi N}^2}{4\pi}$	$\frac{\chi^2}{\text{d.o.f}}$
$ ^1S_0\rangle$	$ ^3S_1\rangle$	$ ^1S_0\rangle$	$ ^3S_1\rangle$	$ ^1S_0\rangle$	$ ^3S_1\rangle$	$ ^1S_0\rangle$	$ ^3S_1\rangle$		
$f_{[2,1]}$	$f_{[1,2]}$	−66.33(4)	−2208(4)	23.73(1)	−5.418(2)	2.68(1)	1.741(3)	12.2(1.4)	0.18
$f_{[1,2]}$	$f_{[1,2]}$	−66.33(4)	−2209(4)	23.73(1)	−5.418(2)	2.68(1)	1.742(3)	12.8(1.2)	0.13
$f_{[2,1]}$	$f_{[2,1]}$	−66.34(4)	−2211(5)	23.73(1)	−5.418(2)	2.68(1)	1.743(3)	$11.9_{-1.5}^{+1.4}$	0.10
$f_{[1,2]}$	$f_{[2,1]}$	−66.34(4)	−2212(4)	23.73(1)	−5.418(2)	2.68(1)	1.744(3)	12.7(1.2)	0.05
$f_{[1,2]}$	−	$-66.4_{-0.5}^{+0.6}$	−	$23.72_{-0.08}^{+0.10}$	−	$2.68_{-0.03}^{+0.02}$	−	$12.4_{-2.3}^{+2.2}$	0.008
−	$f_{[2,1]}$	−	-2222_{-12}^{+14}	−	$-5.416_{-0.003}^{+0.002}$	−	1.749(7)	$18.3_{-8.6}^{+8.4}$	0.04
[34]		−66.5	−2237	23.719	−5.403	2.626	1.749	−	−
[35]		−66.08(13)	−2223(6)	23.748(10)	−5.424(4)	2.75(5)	1.759(5)	−	−
[36]		−66.08(16)	−2223(10)	23.740(20)	−5.419(7)	2.77(5)	1.753(8)	−	−
[23]		−	−2224.7(35)	−	−	−	−	−	−
[43]		−	−2224.575(9)	23.74(2)	−	−	−	−	−
[39]		−	−	−	−	−	−	13.76(8)	−
[40]		−	−	−	−	−	−	13.69(27)	−
[38]		−	−	−	−	−	−	14.23(11)	−
[41]		−	−	−	−	−	−	$13.14_{-0.04}^{+0.07}$	−
[42]		−	−	−	−	−	−	13.6(3)	−

partial-wave analyses of NN observables further confirmed the OPE contribution, reported values around 14 [51] and 12 [52], respectively. In the 1990s, multi-energy partial-wave analyses using the Nijmegen potential on the data of Ref. [23] produced $g_{\pi N}^2/(4\pi) = 13.96(15)^*$ [53] and $13.87(6)^*$ [54]. A later study that replaced the Nijmegen potential with a chiral two-pion-exchange potential obtained $14.02(7)^*$ [55]. Determinations have also been made from the πN data via dispersion relations [39] and the Goldberger-Miyazawa-Oehme sum rule [39, 40], as well as from $N\bar{N}$ data, which

yielded $13.6(3)$ [42]. More recent analyses include a covariance-error partial-wave fit to a selected 3σ -self consistent database, giving $g_{\pi N}^2/(4\pi) = 13.98(11)$ [56], and a Bayesian chiral-effective-field-theory analysis with fully controlled uncertainties, reporting $14.23(11)$ [38]. A theoretical extraction based on pseudoscalar-meson dominance and dispersion relations gives $13.14^{+0.07}_{-0.04}$ [41]. Comprehensive reviews of the history of $g_{\pi N}$ determinations can be found in Refs. [57–60]. We note that the central values extracted in the joint analysis are somewhat smaller than several recent high-precision determinations spreading from about 13.1 to 14.2; this difference indicates the residual contributions beyond the OPE lhc (e.g., two-pion exchange). The extracted values of $g_{\pi N}^2/(4\pi)$ across different expansion orders and schemes exhibit good internal stability. We highlight that the extraction of $g_{\pi N}^2/(4\pi)$ in this work is data-driven within the OPE lhc approximation adopted here, as it relies primarily on the analytic constraints imposed by the lhc and the scattering data. Accordingly, we interpret the extracted $g_{\pi N}^2/(4\pi)$ as an effective measure of the OPE lhc strength within the present truncation, rather than as a competitive high-precision determination of the physical coupling.

IV. SUMMARY

We have applied the generalized ERE with the lhc [1] to low-energy NN scattering, with a focus on the np 1S_0 channel that exhibits an amplitude zero ($\delta = 0$) near $k \simeq 0.35$ GeV (c.m. momentum), which cannot be accommodated using the traditional ERE without changes. Using the np phase shifts of Ref. [23], we performed fits at several expansion orders of Eq. (10), including separate fits to the $|{}^1S_0, I = 1\rangle$ and $|{}^3S_1, I = 0\rangle$ channels and a joint fit constrained by a common πN coupling constant and the coherent scattering length.

The extracted low-energy parameters, including the scattering lengths, effective ranges, and subthreshold poles (a virtual state in 1S_0 and a bound state in 3S_1), are consistent with established determinations and are stable across different expansion orders. Notably, the pseudoscalar πN coupling constant $g_{\pi N}^2/(4\pi)$ is extracted within the OPE lhc approximation adopted here, relying primarily on analytic constraints from the lhc and scattering data. The results, shown in Table I, are consistent with previous determinations from various independent methods, supporting the applicability of the framework in this setting. We find that the central values of $g_{\pi N}^2/(4\pi)$ extracted in the joint analysis tend to be smaller than several recent high-precision determinations around $g_{\pi N}^2/(4\pi) \simeq 14$, implying that residual contributions beyond the OPE lhc (e.g., two-pion exchange) would be needed.

These results indicate that explicitly including the lhc into the ERE not only improves the de-

scription of low-energy scattering observables but also provides a useful framework for constraining the long-range lhc contribution from phase-shift data. The generalized ERE with the lhc thus offers a systematic parameterization for near-threshold systems with light-particle exchanges, enhancing our understanding of the role of OPE in low-energy hadronic interactions. The generalized ERE may be matched to the chiral effective field theory in the region before the opening of the two-pion exchange lhc, which is left to the future work.

ACKNOWLEDGMENTS

We are grateful to Xiong-Hui Cao, Hao-Jie Jing, Bingwei Long, Qi-Fang Lü, and Mao-Jun Yan for useful discussions. This work is supported in part by the National Natural Science Foundation of China under Grants No. 12547115, No. 12125507, No. 12361141819, No. 12447101, and No. 12547111; by the National Key R&D Program of China under Grant No. 2023YFA1606703; and by the Chinese Academy of Sciences under Grant No. YSBR-101. MLD gratefully acknowledges the support of the Peng Huan-Wu Visiting Professorship and the hospitality of the Institute of Theoretical Physics, Chinese Academy of Sciences, where part of this work was completed. UGM also acknowledges the support of the CAS President's International Fellowship Initiative (PIFI) (Grant No. 2025PD0022) and from the European Research Council (ERC) under the European Union's Horizon 2020 research and innovation programme (grant agreement No. 101018170).

[1] M.-L. Du, F.-K. Guo, and B. Wu, Effective-Range Expansion with a Long-Range Force, *Phys. Rev. Lett.* **135**, 011903 (2025), arXiv:2408.09375 [hep-ph].

[2] H. A. Bethe, Theory of the Effective Range in Nuclear Scattering, *Phys. Rev.* **76**, 38 (1949).

[3] J. M. Blatt and J. D. Jackson, On the Interpretation of Neutron-Proton Scattering Data by the Schwinger Variational Method, *Phys. Rev.* **76**, 18 (1949).

[4] S. Navas *et al.* (Particle Data Group), Review of particle physics, *Phys. Rev. D* **110**, 030001 (2024).

[5] M.-Z. Liu, Y.-W. Pan, Z.-W. Liu, T.-W. Wu, J.-X. Lu, and L.-S. Geng, Three ways to decipher the nature of exotic hadrons: Multiplets, three-body hadronic molecules, and correlation functions, *Phys. Rept.* **1108**, 1 (2025), arXiv:2404.06399 [hep-ph].

[6] F.-K. Guo, C. Hanhart, U.-G. Meißner, Q. Wang, Q. Zhao, and B.-S. Zou, Hadronic molecules, *Rev. Mod. Phys.* **90**, 015004 (2018), [Erratum: Rev.Mod.Phys. 94, 029901 (2022)], arXiv:1705.00141 [hep-ph].

[7] H.-X. Chen, W. Chen, X. Liu, Y.-R. Liu, and S.-L. Zhu, An updated review of the new hadron states,

Rept. Prog. Phys. **86**, 026201 (2023), arXiv:2204.02649 [hep-ph].

[8] L. Meng, B. Wang, G.-J. Wang, and S.-L. Zhu, Chiral perturbation theory for heavy hadrons and chiral effective field theory for heavy hadronic molecules, Phys. Rept. **1019**, 1 (2023), arXiv:2204.08716 [hep-ph].

[9] N. Brambilla, S. Eidelman, C. Hanhart, A. Nefediev, C.-P. Shen, C. E. Thomas, A. Vairo, and C.-Z. Yuan, The XYZ states: experimental and theoretical status and perspectives, Phys. Rept. **873**, 1 (2020), arXiv:1907.07583 [hep-ex].

[10] V. Baru, X.-K. Dong, M.-L. Du, A. Filin, F.-K. Guo, C. Hanhart, A. Nefediev, J. Nieves, and Q. Wang, Effective range expansion for narrow near-threshold resonances, Phys. Lett. B **833**, 137290 (2022), arXiv:2110.07484 [hep-ph].

[11] X.-K. Dong, F.-K. Guo, and B.-S. Zou, A survey of heavy-heavy hadronic molecules, Commun. Theor. Phys. **73**, 125201 (2021), arXiv:2108.02673 [hep-ph].

[12] X.-K. Dong, F.-K. Guo, and B.-S. Zou, A survey of heavy-antiheavy hadronic molecules, Progr. Phys. **41**, 65 (2021), arXiv:2101.01021 [hep-ph].

[13] M.-L. Du, F.-K. Guo, and B. Wu, Effective range expansion with the left-hand cut and its application to the $T_{cc}(3875)$, in *11th International Workshop on Chiral Dynamics* (2025) arXiv:2502.19774 [hep-ph].

[14] E. Epelbaum and U.-G. Meißner, Chiral dynamics of few- and many-nucleon systems, Ann. Rev. Nucl. Part. Sci. **62**, 159 (2012), arXiv:1201.2136 [nucl-th].

[15] W.-J. Wang, B. Wu, M.-L. Du, and F.-K. Guo, Effective Range Expansion with the Left-Hand Cut: Higher Order Improvements, (2026), arXiv:2601.04989 [hep-ph].

[16] X. Zhang, H.-L. Fu, F.-K. Guo, and H.-W. Hammer, Neutron scattering off one-neutron halo nuclei in halo effective field theory, Phys. Rev. C **108**, 044304 (2023), arXiv:2308.12815 [nucl-th].

[17] M.-L. Du, A. Filin, V. Baru, X.-K. Dong, E. Epelbaum, F.-K. Guo, C. Hanhart, A. Nefediev, J. Nieves, and Q. Wang, Role of Left-Hand Cut Contributions on Pole Extractions from Lattice Data: Case Study for $T_{cc}(3875)^+$, Phys. Rev. Lett. **131**, 131903 (2023), arXiv:2303.09441 [hep-ph].

[18] R. A. Arndt, L. D. Roper, R. A. Bryan, R. B. Clark, B. J. VerWest, and P. Signell, Nucleon-Nucleon Partial Wave Analysis to 1 GeV, Phys. Rev. D **28**, 97 (1983).

[19] V. G. J. Stoks, R. A. M. Klomp, C. P. F. Terheggen, and J. J. de Swart, Construction of high quality NN potential models, Phys. Rev. C **49**, 2950 (1994), arXiv:nucl-th/9406039.

[20] T. A. Rijken and V. G. J. Stoks, Soft two meson exchange nucleon-nucleon potentials. II. one pair and two pair diagrams, Phys. Rev. C **54**, 2869 (1996), arXiv:nucl-th/9509031.

[21] P. Reinert, H. Krebs, and E. Epelbaum, Semilocal momentum-space regularized chiral two-nucleon potentials up to fifth order, Eur. Phys. J. A **54**, 86 (2018), arXiv:1711.08821 [nucl-th].

[22] R. A. Arndt, I. I. Strakovsky, and R. L. Workman, Nucleon nucleon elastic scattering to 3 GeV, Phys. Rev. C **62**, 034005 (2000), arXiv:nucl-th/0004039.

[23] V. G. J. Stoks, R. A. M. Klomp, M. C. M. Rentmeester, and J. J. de Swart, Partial wave analysis of all nucleon-nucleon scattering data below 350 MeV, Phys. Rev. C **48**, 792 (1993).

[24] G. F. Chew and S. Mandelstam, Theory of low-energy pion pion interactions, *Phys. Rev.* **119**, 467 (1960).

[25] J. A. Oller, *A Brief Introduction to Dispersion Relations*, SpringerBriefs in Physics (Springer, 2019).

[26] M. L. Goldberger and S. B. Treiman, Conserved Currents in the Theory of Fermi Interactions, *Phys. Rev.* **110**, 1478 (1958).

[27] N. Fettes, U.-G. Meißner, and S. Steininger, Pion-nucleon scattering in chiral perturbation theory. 1. Isospin symmetric case, *Nucl. Phys. A* **640**, 199 (1998), arXiv:hep-ph/9803266.

[28] R. B. Wiringa, V. G. J. Stoks, and R. Schiavilla, An Accurate nucleon-nucleon potential with charge independence breaking, *Phys. Rev. C* **51**, 38 (1995), arXiv:nucl-th/9408016.

[29] E. Epelbaum, H. Krebs, and U.-G. Meißner, Precision nucleon-nucleon potential at fifth order in the chiral expansion, *Phys. Rev. Lett.* **115**, 122301 (2015), arXiv:1412.4623 [nucl-th].

[30] E. Epelbaum, H. Krebs, and U.-G. Meißner, Improved chiral nucleon-nucleon potential up to next-to-next-to-next-to-leading order, *Eur. Phys. J. A* **51**, 53 (2015), arXiv:1412.0142 [nucl-th].

[31] J.-X. Lu, C.-X. Wang, Y. Xiao, L.-S. Geng, J. Meng, and P. Ring, Accurate Relativistic Chiral Nucleon-Nucleon Interaction up to Next-to-Next-to-Leading Order, *Phys. Rev. Lett.* **128**, 142002 (2022), arXiv:2111.07766 [nucl-th].

[32] R. Machleidt, K. Holinde, and C. Elster, The Bonn Meson Exchange Model for the Nucleon Nucleon Interaction, *Phys. Rept.* **149**, 1 (1987).

[33] K. Schoen, D. L. Jacobson, M. Arif, P. R. Huffman, T. C. Black, W. M. Snow, S. K. Lamoreaux, H. Kaiser, and S. A. Werner, Precision neutron interferometric measurements and updated evaluations of the n - p and n - d coherent neutron scattering lengths, *Phys. Rev. C* **67**, 044005 (2003).

[34] V. A. Babenko and N. M. Petrov, Determination of low-energy parameters of neutron-proton scattering on the basis of modern experimental data from partial-wave analyses, *Phys. Atom. Nucl.* **70**, 669 (2007), arXiv:0704.1024 [nucl-th].

[35] O. Dumbrajs, R. Koch, H. Pilkuhn, G. Oades, H. Behrens, J. De Swart, and P. Kroll, Compilation of coupling constants and low-energy parameters, *Nuclear Physics B* **216**, 277 (1983).

[36] R. Machleidt, High-precision, charge-dependent Bonn nucleon-nucleon potential, *Physical Review C* **63**, 024001 (2001), nucl-th/0006014.

[37] E. Epelbaum, H.-W. Hammer, and U.-G. Meißner, Modern Theory of Nuclear Forces, *Rev. Mod. Phys.* **81**, 1773 (2009), arXiv:0811.1338 [nucl-th].

[38] P. Reinert, H. Krebs, and E. Epelbaum, Precision determination of pion-nucleon coupling constants using effective field theory, *Phys. Rev. Lett.* **126**, 092501 (2021), arXiv:2006.15360 [nucl-th].

[39] R. Arndt, W. Briscoe, I. Strakovsky, and R. Workman, Extended partial-wave analysis of πN scattering data, *Phys. Rev. C* **74**, 045205 (2006), arXiv:nucl-th/0605082 [nucl-th].

[40] V. Baru, C. Hanhart, M. Hoferichter, B. Kubis, A. Nogga, and D. Phillips, Precision calculation of threshold $\pi^- d$ scattering, πN scattering lengths, and the GMO sum rule, *Nucl. Phys. A* **872**, 69 (2011), arXiv:1107.5509 [nucl-th].

- [41] E. Ruiz Arriola and P. Sanchez-Puertas, Pseudoscalar meson dominance, the pion-nucleon coupling constant and the Goldberger-Treiman discrepancy, (2025), [arXiv:2507.22726 \[hep-ph\]](https://arxiv.org/abs/2507.22726).
- [42] R. Timmermans, T. Rijken, and J. de Swart, Determination of the charged pion coupling constant from data on the charge exchange reaction $\bar{p}p \rightarrow \bar{n}n$, *Phys. Rev. Lett.* **67**, 1074 (1991).
- [43] R. Navarro Pérez, J. Amaro, and E. Ruiz Arriola, Coarse-grained potential analysis of neutron-proton and proton-proton scattering below the pion production threshold, *Phys. Rev. C* **88**, 064002 (2013), [arXiv:1310.2536 \[nucl-th\]](https://arxiv.org/abs/1310.2536).
- [44] H. A. Bethe, The Meson Theory of Nuclear Forces I. General Theory, *Phys. Rev.* **57**, 260 (1940).
- [45] H. A. Bethe, The Meson Theory of Nuclear Forces. Part II. Theory of the Deuteron, *Phys. Rev.* **57**, 390 (1940).
- [46] Y. Nambu, Axial vector current conservation in weak interactions, *Phys. Rev. Lett.* **4**, 380 (1960).
- [47] M. L. Goldberger and S. B. Treiman, Decay of the π meson, *Phys. Rev.* **110**, 1178 (1958).
- [48] G. F. Chew, Proposal for Determining the Pion-Nucleon Coupling Constant from the Angular Distribution for Nucleon-Nucleon Scattering, *Phys. Rev.* **112**, 1380 (1958).
- [49] P. Cziffra, M. H. MacGregor, M. J. Moravcsik, and H. P. Stapp, Modified Analysis of Nucleon-Nucleon Scattering. I. Theory and p - p Scattering at 310 Mev, *Phys. Rev.* **114**, 880 (1959).
- [50] M. H. MacGregor, M. J. Moravcsik, and H. P. Stapp, Modified Analysis of Nucleon-Nucleon Scattering. II. Completed Analysis of p - p Scattering at 310 Mev, *Phys. Rev.* **116**, 1248 (1959).
- [51] P. S. Signell, Quantitative Evidence of One-Pion Exchange Effects in p - p Scattering, *Phys. Rev. Lett.* **5**, 474 (1960).
- [52] M. H. MacGregor, R. A. Arndt, and A. A. Dubow, Determination of the Nucleon-Nucleon Elastic Scattering Matrix. I. Phase-Shift Analysis of Experiments Near 140 MeV, *Phys. Rev.* **135**, B628 (1964).
- [53] R. A. M. Klomp, V. G. J. Stoks, and J. J. de Swart, Determination of the $NN\pi$ coupling constants in NN partial wave analyses, *Phys. Rev. C* **44**, R1258 (1991).
- [54] V. G. Stoks, R. Timmermans, and J. J. de Swart, On the pion-nucleon coupling constant, *Phys. Rev. C* **47**, 512 (1993), [arXiv:nucl-th/9211007 \[nucl-th\]](https://arxiv.org/abs/nucl-th/9211007).
- [55] M. C. M. Rentmeester, R. G. E. Timmermans, J. L. Friar, and J. J. de Swart, Chiral two pion exchange and proton proton partial wave analysis, *Phys. Rev. Lett.* **82**, 4992 (1999), [arXiv:nucl-th/9901054 \[nucl-th\]](https://arxiv.org/abs/nucl-th/9901054).
- [56] R. Navarro Pérez, J. Amaro, and E. Ruiz Arriola, Precise Determination of Charge Dependent Pion-Nucleon-Nucleon Coupling Constants, *Phys. Rev. C* **95**, 064001 (2017), [arXiv:1606.00592 \[nucl-th\]](https://arxiv.org/abs/1606.00592).
- [57] J. de Swart, M. Rentmeester, and R. Timmermans, The Status of the pion-nucleon coupling constant, (1998), [arXiv:nucl-th/9802084 \[nucl-th\]](https://arxiv.org/abs/nucl-th/9802084).
- [58] M. Sainio, Pion nucleon coupling constant: Working group summary, (1999), [arXiv:hep-ph/9912337 \[hep-ph\]](https://arxiv.org/abs/hep-ph/9912337).
- [59] D. Bugg, The pion nucleon coupling constant, *Eur. Phys. J. C* **33**, 505 (2004).
- [60] E. Matsinos, A brief history of the pion-nucleon coupling constant, (2019), [arXiv:1901.01204 \[nucl-th\]](https://arxiv.org/abs/1901.01204).